Molecular Physics
Vol. 00, No. 00, Month 200x, 1–17

RESEARCH ARTICLE

On the difference between a point multipole and an equivalent linear arrangement of point charges in force field models for vapour-liquid equilibria. Partial charge based models for 59 real fluids

Cemal Engin[a], Jadran Vrabec[b*] and Hans Hasse[a]

[a] *Laboratory of Engineering Thermodynamics, University of Kaiserslautern, Erwin-Schrödinger-Str. 44, 67633 Kaiserslautern, Germany*;
[b] *Thermodynamics and Energy Technology, University of Paderborn, Warburger Str. 100, 33098 Paderborn, Germany*

(*Received 00 Month 200x; final version received 00 Month 200x*)

The replacement of a point dipole and a point quadrupole by a corresponding linear arrangement of two point charges ($+q$, $-q$) and accordingly three point charges ($+q$, $-2q$, $+q$) is studied with respect to vapour-liquid equilibria. The dependence of saturated liquid density, vapour pressure and heat of vaporisation on the choice of the distance d between the charges in the point charge arrangement is analysed. For the studied dipolar two-centre Lennard-Jones (2CLJD) and quadrupolar two-centre Lennard-Jones (2CLJQ) models, d/σ between 1/15 and 1/20 is a reasonable compromise between numerical and physical accuracy, where σ is the Lennard-Jones size parameter. The results are used to derive validated partial charge based models of 59 real fluids from previously published point dipole and point quadrupole based models.

Keywords: molecular modelling; polar interactions; vapour-liquid equilibrium

1. Introduction

Lennard-Jones (LJ) based molecular models with superimposed electrostatic sites are a widely used class of force fields for molecular simulations of thermophysical properties of fluids. Stoll et al. [1] and Vrabec et al. [2] have modelled 38 real fluids with rigid two-centre LJ (2CLJ) models with a superimposed point dipole and 21 fluids with a superimposed point quadrupole. The four model parameters (LJ size σ and energy ϵ, elongation L, i.e. distance between the LJ sites, and dipole moment μ or quadrupole moment Q) were determined from a fit to correlations of experimental vapour-liquid equilibrium (VLE) data. Polar 2CLJ models strongly simplify the intermolecular interactions, e.g. the asymmetry of the molecules is neglected and the polar interaction is always aligned along the main molecular axis. Also the polarizability, which is often assumed to be a crucial molecular property for thermodynamics, is only implicitly considered by LJ interaction sites. Furthermore, the internal degrees of freedom are neglected as the polar 2CLJ models are rigid. However, it has been shown in many applications [3–7] that these models have an excellent predictive power for various properties, including transport data.

*Corresponding author. Email: jadran.vrabec@upb.de

ISSN: 0040-5167 print/ISSN 1754-2278 online

DOI: 10.1080/0040516YYxxxxxxxx
http://www.informaworld.com

Therefore, it is not in the scope of this work to study the performance of these molecular models with respect to their descriptive or predictive capabilities.

Most molecular simulation programs do not support point multipole sites, but only point charges [8, 9]. Despite the fact that the point multipoles are computationally significantly less demanding than a corresponding arrangement of point charges [10], replacing point multipoles by a set of point charges can therefore be a necessity. From the physical perspective, it should be noted that multipoles are often better suited to describe the electrostatic molecular interactions [11]. Along these lines, Coen et al. [12] have studied point dipoles and analogous point charge sets for protein-protein interactions.

Because there is one degree of freedom for replacing point dipoles and point quadrupoles by point charges, this study was carried out to rationalize how this is best done and to give a recommendation for a point charge version of the multipolar models of Stoll et al. [1] and Vrabec et al. [2].

2. Replacing point multipoles by point charge arrangements

The symmetric two-centre LJ plus point dipole (2CLJD) or point quadrupole (2CLJQ) pair potentials are composed of two identical LJ sites a distance L apart plus a point dipole of moment μ or a point quadrupole of moment Q that is placed in the geometric centre of the molecular model and is aligned in the direction of the axis A connecting the two LJ sites. These point multipoles can be replaced by a close arrangement of two point charges $(+q, -q)$ in case of a point dipole or three point charges $(+q, -2q, +q)$ in the case of a point quadrupole.

2.1. *Replacement of a point quadrupole by three point charges*

The charge magnitude q in the arrangement $(+q, -2q, +q)$ can be either negative or positive, depending on the sign of the quadrupole moment Q. To mimic the point quadrupole of a 2CLJQ model, the central charge has to be placed in the geometric centre of the model and the two other charges on the axis A in a distance $\pm\, d$ from the centre. Note that the sign of the quadrupole moment does not play a role for pure component properties as studied in the present work, but it generally does in mixtures [5]. This charge distribution has a quadrupole moment [13, 14]

$$Q = 2qd^2 \tag{1}$$

and the octupole moment is zero. For replacing the point quadrupole by that type of point charge arrangement, either one of the parameters d or q can be specified and Equation (1) has to be used to determine the other parameter for the given value of Q. That choice is less trivial then it might seem. E.g. Ungerer et al. [15] have distributed the three charges on the molecular axis at $\pm\, 0.5$ Å from the centre of the CO_2 model by Vrabec et al. [2], i.e. they used $d/\sigma \approx 1/6$, and obtained unfavourable VLE results.

In this work, the influence of the choice of d on the saturated liquid density, vapour pressure and heat of vaporisation was investigated in detail for two selected substances, namely Chlorine (Cl_2) and the refrigerant 1,2-Dichloro-1,1,2,2-tetrafluoroethane (CF_2Cl-CF_2Cl). Both the quadrupole moment Q and the elongation L increase from Cl_2 to CF_2Cl-CF_2Cl, cf. Table 1. In a first step, the temperature was set to $0.7\, T_c$, where T_c is the critical temperature of the substance, while d was varied and the quadrupolar moment was kept constant. The results are

shown in Figures 1 and 2. For small values of d (corresponding to large values of q), numerical problems in the evaluation of the force field during molecular simulation become apparent. These are due to the contributions of point charges with a very large magnitude that have an alternating sign. Numerically, this translates to subtractions of large numbers. On the other hand, for large values of d, the error from approximating the point quadrupole by a spatially elongated point charge arrangement becomes important. This is visualized in Figure 3, where an equipotential line for a point quadrupole and for an according point charge arrangement with $d/\sigma = 1/3$ is shown. It can be seen that the two electrostatic models deviate significantly from each other for this separation. Thus, there must be an optimum for the choice of d, for which the replacement is best suited for representing VLE properties. From Figures 1 and 2 it can be seen that this optimum is in the range of $1/20 \leq d/\sigma \leq 1/15$.

For Cl_2, the present simulations were done with two different molecular simulation codes to check for generality and reproducibility of the results. These codes were our own group's software $ms2$ [10] and the Gibbs Ensemble Monte-Carlo (GEMC) code by Errington [16]. The simulation details are given in the Appendix. As can be seen in Figure 1, if d is too small, the results from the point charge model may differ strongly from those of the point quadrupole model, which is clearly visible from the results of the GEMC code. $ms2$ proved to be numerically more robust. This observation was confirmed by additional simulations for distances $d/\sigma = 1/40,\ 1/60,\ 1/80$ and $1/150$ in the case of CF_2Cl-CF_2Cl, which is more suitable for this study because of its very large quadrupole moment $Q = 11.456\,\text{DÅ}$. No significant increase was visible in the relative error. In Figure 2, only the data points for the separations $d = \sigma/40$ and $\sigma/60$ are plotted for clarity. On the other hand, for large values of d, also large errors occur, but they are similar for both codes, because they are due to the inappropriateness of the physical approximation of the point quadrupole by three point charges.

Figure 4 shows a comparison of the results from the point quadrupole model and two versions of the corresponding point charge model ($d = \sigma/15$ and $\sigma/20$) for the VLE properties of $CFCl_2$-CF_3 in the temperature range $0.65 < T/T_c < 0.95$. The CF_2Cl-CF_2Cl model is very sensitive to variations in d, because of its large quadrupole moment and the wide separation $L = 0.8\,\sigma$ between the LJ sites. Both point charge models are in very good agreement with the original model. All model versions agree better with each other for higher temperatures, due to the fact that the effect of the quadrupole-quadrupole interaction decreases inversely proportional to $k_B\,T$ [14, 17]. This result is expected to be valid also in the case of the point dipole replacement, because the dipole-dipole interaction has the same proportionality $1/(k_B\,T)$ [14, 17] as discussed below.

To study whether these results can be generalized, all 21 quadrupolar models of Vrabec et al. [2] were simulated here. Again, two versions of the point charge model were investigated: $d = \sigma/15$ and $\sigma/20$. The simulations were carried out with $ms2$ only.

For each substance, the VLE results based on two versions of the point charge models were compared to those from the original point quadrupole models of Vrabec et al. [2]. The comparison is summarized in Figure 5, the model parameters are given in Table 1. Generally, slightly better results were obtained for $d = \sigma/20$, which is therefore recommended. Note that this recommendation is not independent on the numerical robustness of the simulation code, e.g. Figure 1 indicates that $\sigma/10 \leq d \leq \sigma/15$ may be a better choice for the GEMC code [16] used here.

Figure 5 shows that the point charge arrangement with $d = \sigma/20$ rarely deviates from the original point quadrupole model by more than 0.1 % for the saturated

liquid density and 0.4 % for the heat of vaporisation. These numbers are well within the range of typical deviations from experimental data. The corresponding number for the vapour pressure is 5 % and, hence, corresponds to the typical deviation from experimental data for that more sensitive property.

2.2. *Replacement of a point dipole by two point charges*

The point dipole of 2CLJD models was replaced by two point charges $(+q, -q)$, which were positioned symmetrically on both sides of the geometric centre along the axis A, separated by the distance d. This charge distribution has a dipole moment [13, 14]

$$\mu = q\,d \tag{2}$$

and the quadrupole moment is zero. Again, the two parameters q and d can vary to specify a given value of the dipole moment μ. The equipotential lines for a point dipole and a point charge representation with the same dipole moment and a separation of $d = \sigma/3$ is shown in Figure 6.

As in the study above, three dipolar substances with medium to large dipole moments and small to large elongations L, namely 1,1-Difluoroethylene (CF_2=CH_2), 1,1,1-Trifluoro-2-bromo-2-chloroethane (CF_3-CHClBr) and Methylchloride (CH_3Cl), were selected to investigate the dependence of the VLE properties on the separation d. Figures 7 to 9 show that the optimum distance is again in the range of $\sigma/20 \leq d \leq \sigma/15$. The numerical errors for short distances are not as dominant as for the point quadrupole, because the value of the charge magnitude q increases only linearly with the decreasing distance d and not quadratic as for the point quadrupole, cf. Equations (1) and (2) and Tables 1 and 2.

These findings were applied to 38 2CLJD models by Stoll et al. [1] for the recommended distance $d = \sigma/20$. For each substance, the VLE results based on the point charge model were compared to those from the original point dipole model of Stoll et al. [1]. This comparison is summarized in Figure 10, the model parameters are given in Table 2. Figure 10 shows that the point charge arrangement with $d = \sigma/20$ rarely deviates from the original point dipole model by more than 0.3 % for the saturated liquid density and for the heat of vaporisation. The corresponding number for the vapour pressure is 5 %.

3. Conclusions

The substitution of point multipoles of 2CLJD and 2CLJQ potentials by linear point charge arrangements was studied. For both the point dipole and the point quadrupole, a separation of $d = \sigma/20$ between the point charges is recommended to maintain the quality of the original models with respect to saturated liquid density, vapour pressure and heat of vaporisation. For the recommended distance of $d = \sigma/20$, the deviations from the original models of the mentioned thermodynamic VLE properties were analysed for 38 dipolar and 21 quadrupolar models and the parameters for the corresponding point charge models were given. The deviations for saturated liquid density and heat of vaporisation rarely exceeded 0.3 % and 0.4 %, respectively. The corresponding number for the vapour pressure is 5 % and is thus in the range of typical deviations from experimental data for this sensitive property.

Acknowledgments

We gratefully acknowledge support of this work by Deutsche Forschungsgemeinschaft. This work was carried out under the auspices of the Boltzmann-Zuse Society (BZS) of Computational Molecular Engineering. The simulations were performed on the national super computer NEC Nehalem Cluster at the High Performance Computing Center Stuttgart (HLRS) under the grant MMHBF2.

References

[1] J. Stoll, J. Vrabec and H. Hasse, J. Chem. Phys. **119**, 11396 (2003).
[2] J. Vrabec, J. Stoll and H. Hasse, J. Phys. Chem. B **105**, 12126 (2001).
[3] D. Möller and J. Fischer, Fluid Phase Equilib. **100**, 35 (1994).
[4] G. A. Fernandez, J. Vrabec and H. Hasse, Int. J. Thermophys. **26**, 1389 (2005).
[5] J. Vrabec, J. Stoll and H. Hasse, Mol. Sim. **31**, 215 (2005).
[6] J. Stoll, J. Vrabec and H. Hasse, AIChE J. **49**, 2187 (2003).
[7] J. Vrabec, G. K. Kedia and H. Hasse, Cryogenics **45**, 253 (2005).
[8] B. Hess, C. Kutzner, D. van der Spoel and E. Lindahl, J. Chem. Theory Comput. **4**, 435 (2008).
[9] Towhee monte carlo molecular simulation code, http://towhee.sourceforge.net.
[10] S. Deublein, B. Eckl, J. Stoll, S. V. Lishchuk, G. Guevara, C. W. Glass, T. Merker, M. Bernreuther, J. Vrabec and H. Hasse, Comp. Phys Commun. (2011), in press, doi:10.1016/j.cpc.2011.04.026.
[11] A. J. Stone, Science **321**, 787 (2008).
[12] C. J. Coen, J. Newman, H. W. Blanch and J. M. Prausnitz, J. Coll. Int. Sci. **177**, 276 (1996).
[13] W. Nolting, *Grundkurs Theoretische Physik 3: Elektrodynamik* (Springer-Verlag, Berlin, Heidelberg, 2007).
[14] J. M. Prausnitz, R. N. Lichtenthaler and E. G. de Azevedo, *Molecular Thermodynamics of Fluid-Phase Equilibria*, p. 60 (Prentice-Hall, Englewood Cliffs, New Jersey, 1999).
[15] P. Ungerer, A. Wender, G. Demoulin, E. Bourasseau and P. Mougin, Mol. Sim. **30**, 631 (2004).
[16] Errington monte carlo molecular simulation code, http://kea.princeton.edu/jerring/gibbs.
[17] J. O. Hirschfelder, C. F. Curtiss and R. B. Bird, *Molecular theory of gases and liquids*, p. 835 (John Wiley and Sons, New York, London, Sydney, 1954).
[18] J. Vrabec and H. Hasse, Mol. Phys. **100**, 3375 (2002).
[19] M. P. Allen and D. J. Tildesley, *Computer simulations of liquids*, p. 162 (Clarendon Press, Oxford, 1987).
[20] A. Z. Panagiotopoulos, Mol. Phys. **61**, 813 (1987).
[21] J. Stoll, *Molecular Models for the Prediction of Thermophysical Properties of Pure Fluids and Mixtures*, Reihe 3, Nr. 836 (VDI-Verlag, Düsseldorf, 2005).

Appendix A: Simulation details

The VLE calculations with *ms*2 were done employing the Grand Equilibrium method [18]. The code structure of *ms*2 is described in [10], as a compiler Intel ifort 11.1 was used and the simulations were executed on a cluster of Intel Xeon E5560 processors. The fluid was equilibrated over up to $26 \cdot 10^6$ MC steps using 864 particles and the production run went up to $172 \cdot 10^6$ MC steps. The electrostatic contributions were calculated by the reaction field method [19] with tinfoil boundary conditions. The cut-off radius was chosen to be $5\,\sigma$ for all models with few exceptions and long-range corrections for energy and pressure were applied. If $5\,\sigma$ exceeded half of the simulation box length, the value of the cut-off radius was adopted accordingly. The results for Cl_2, $CF_2{=}CH_2$ and CF_3-CHClBr were checked by a GEMC code [16, 20], where the total number of particles in both volumes was 1000. The systems were equilibrated over up to $15 \cdot 10^6$ MC steps and the number of production steps was up to $80 \cdot 10^6$. The electrostatic long range contributions were calculated in this case with the Ewald summation method [19]. The cut-off radius for the LJ interactions corresponded to half of the respective box length and long-range corrections for energy and pressure were applied.

Table 1. Molecular parameters of 2CLJQ type models for 21 substances. The quadrupole was modelled either by a point quadrupole with the moment Q (numbers were taken from Vrabec et al. [2], except for CF_2Cl-CF_2Cl where the numbers were taken from Stoll [21]) or as a corresponding point charge arrangement with $d = \sigma/20$.

#	fluid	(ϵ/k_B) / K	σ / Å	L/σ	Q / DÅ	q / e	d / Å
1	F_2	52.147	2.8258	0.5000	0.8920	4.652	0.14129
2	Cl_2	160.86	3.4016	0.5826	4.2356	15.242	0.17008
3	Br_2	236.76	3.5546	0.6126	4.8954	16.136	0.17773
4	I_2	371.47	3.7200	0.7200	5.6556	17.021	0.18600
5	N_2	34.897	3.3211	0.3151	-1.4397	-5.435	0.16606
6	O_2	43.183	3.1062	0.3123	-0.8081	-3.488	0.15531
7	CO_2	133.22	2.9847	0.8100	-3.7938	-17.736	0.14924
8	CS_2	257.68	3.6140	0.7418	3.8997	12.435	0.18070
9	C_2H_6	136.99	3.4896	0.6809	-0.8277	-2.831	0.17448
10	C_2H_4	76.950	3.7607	0.3376	4.3310	12.754	0.18804
11	C_2H_2	79.890	3.5742	0.3637	5.0730	16.539	0.17871
12	C_2F_6	110.19	4.1282	0.6600	-8.4943	-20.759	0.20641
13	C_2F_4	106.32	3.8611	0.5800	-7.0332	-19.648	0.19306
14	C_2Cl_4	211.11	4.6758	0.5672	-16.143	-30.751	0.23379
15	propadiene	170.52	3.6367	0.6863	5.1637	16.261	0.18184
16	propyne	186.43	3.5460	0.8000	-5.7548	-19.061	0.17730
17	SF_6	118.96	3.9615	0.6658	8.0066	21.248	0.19808
18	CF_4	59.235	3.8812	0.3582	5.1763	14.311	0.19406
19	CCl_4	142.14	4.8471	0.3496	14.346	25.431	0.24236
20	propylene	150.78	3.8169	0.6553	5.9387	16.977	0.19085
21	CF_2Cl-CF_2Cl	183.26	4.3772	0.8000	11.456	24.902	0.21886

Table 2. Molecular parameters of 2CLJD type models for 38 substances. The dipole was modelled either by a point dipole with the moment μ (numbers were taken from Stoll et al. [1]) or as a corresponding point charge arrangement with $d = \sigma/20$.

#	fluid	(ϵ/k_B) / K	σ / Å	L/σ	μ / D	q / e	d / Å
1	CO	36.897	3.3009	0.3455	0.7378	0.9308	0.08253
2	R11	224.15	4.0213	0.83	2.7009	2.7977	0.10051
3	R12	185.66	3.8286	0.8541	2.3219	2.5293	0.09557
4	R13	145.95	3.6184	0.8495	1.8261	2.1016	0.09046
5	R13B1	170.32	3.6817	0.9119	2.0478	2.3162	0.09205
6	R22	177.43	3.4682	0.8997	2.2667	2.7216	0.08671
7	R23	123.56	3.2643	0.7864	2.1607	2.7563	0.08161
8	R41	137.64	3.0382	0.8074	1.8850	2.5835	0.07596
9	R123	221.75	4.0530	0.9130	3.7002	3.8016	0.10133
10	R124	192.25	3.8852	1	3.2190	3.4502	0.09713
11	R141b	231.43	4.0209	0.8957	3.1484	3.2604	0.10053
12	R142b	193.68	3.8404	0.9029	2.9610	3.2107	0.09601
13	R143a	165.04	3.5960	0.9843	2.7470	3.1811	0.08990
14	R152a	182.01	3.5168	0.9419	2.7354	3.2390	0.08792
15	CH_3Cl	186.57	3.3409	0.7700	2.0217	2.5200	0.08352
16	CH_3Br	213.81	3.4557	0.7566	1.8536	2.2337	0.08639
17	CH_3I	232.86	3.6367	0.7447	2.4983	2.8607	0.09092
18	CH_2BrCl	274.49	3.5838	0.9951	3.1998	3.7179	0.08960
19	$CHCl_3$	265.29	3.8153	0.9907	3.3920	3.7024	0.09538
20	$CHBr_3$	357.41	4.0575	0.9716	3.5204	3.6130	0.10144
21	$CHFCl_2$	220.69	3.6522	0.9418	2.7852	3.1755	0.09131
22	$CBrClF_2$	212.23	3.8560	0.9325	2.6786	2.8927	0.09640
23	$CBrCl_3$	305.34	4.1366	0.9638	3.6313	3.6554	0.10342
24	CH_2F-CH_3	176.84	3.3968	0.9128	2.4110	2.9557	0.08492
25	$CHCl_2$-CH_2Cl	286.36	4.0768	0.9835	4.2974	4.3896	0.10192
26	$CHCl_2$-CH_3	255.24	3.8579	0.9885	3.5236	3.8033	0.09645
27	CCl_3-CH_3	253.75	4.2224	0.8265	3.5019	3.4537	0.10556
28	CH_2Cl-CCl_3	292.86	4.3282	0.9533	4.7919	4.6102	0.10821
29	CH_2F-CCl_3	259.97	4.1262	0.9323	4.3049	4.3444	0.10316
30	CF_3-$CHClBr$	151.78	4.6727	0.4430	3.7380	3.3312	0.11682
31	CCl_3-CF_2Cl	258.25	4.3651	0.9746	4.7132	4.4964	0.10913
32	$CHF{=}CH_2$	155.74	3.3552	0.8200	1.6565	2.0560	0.08388
33	$CHCl{=}CH_2$	181.16	3.6875	0.6793	2.1078	2.3803	0.09219
34	$CHCl{=}CF_2$	193.24	3.6501	0.9451	2.7449	3.1317	0.09125
35	$CFCl{=}CF_2$	181.71	3.7438	0.9488	2.8408	3.1597	0.09360
36	$CFBr{=}CF_2$	218.12	3.8290	0.9369	2.5273	2.7485	0.09573
37	$CF_2{=}CH_2$	71.963	3.7848	0.3927	2.3643	2.6014	0.09462
38	CH_2Br-CH_3	255.75	3.6769	1	2.9425	3.3326	0.09192

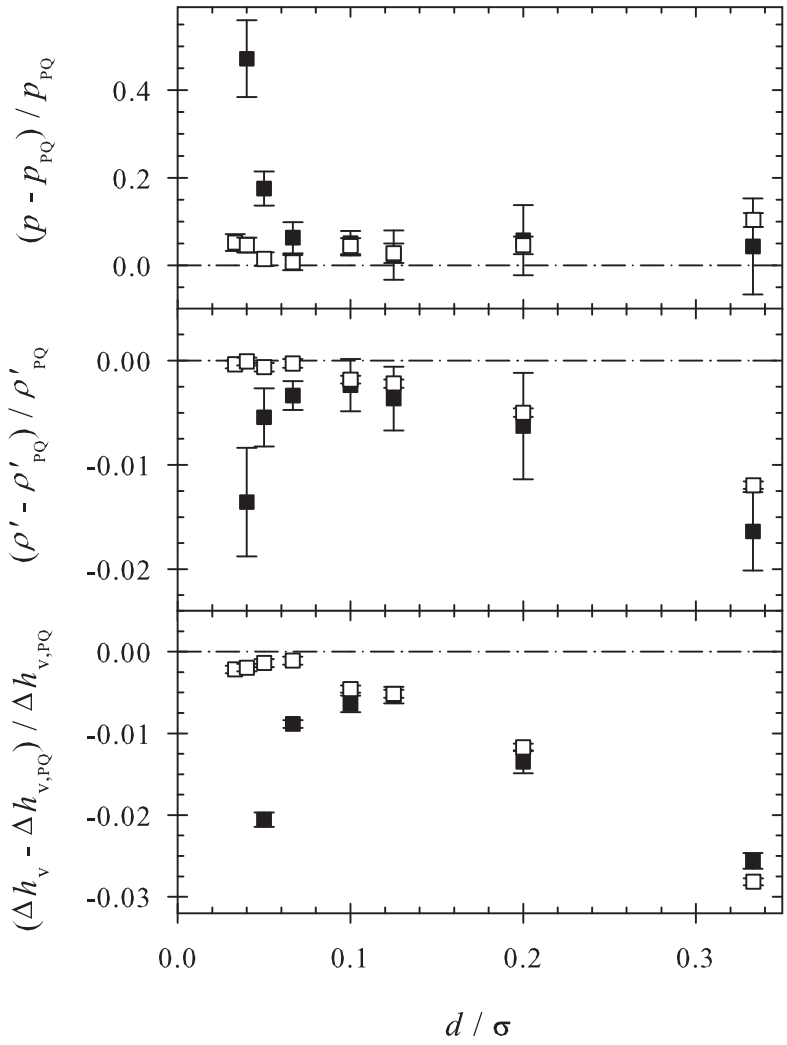

Figure 1. Relative deviations of VLE properties between the point quadrupole (subscript PQ) and the corresponding point charge model for Chlorine (Cl_2) at $T/T_c = 0.7$. The deviations are plotted over the separation d between the point charges. Full symbols: GEMC code [16], empty symbols: *ms*2 code [10]. Top: vapour pressure, centre: saturated liquid density, bottom: heat of vaporisation.

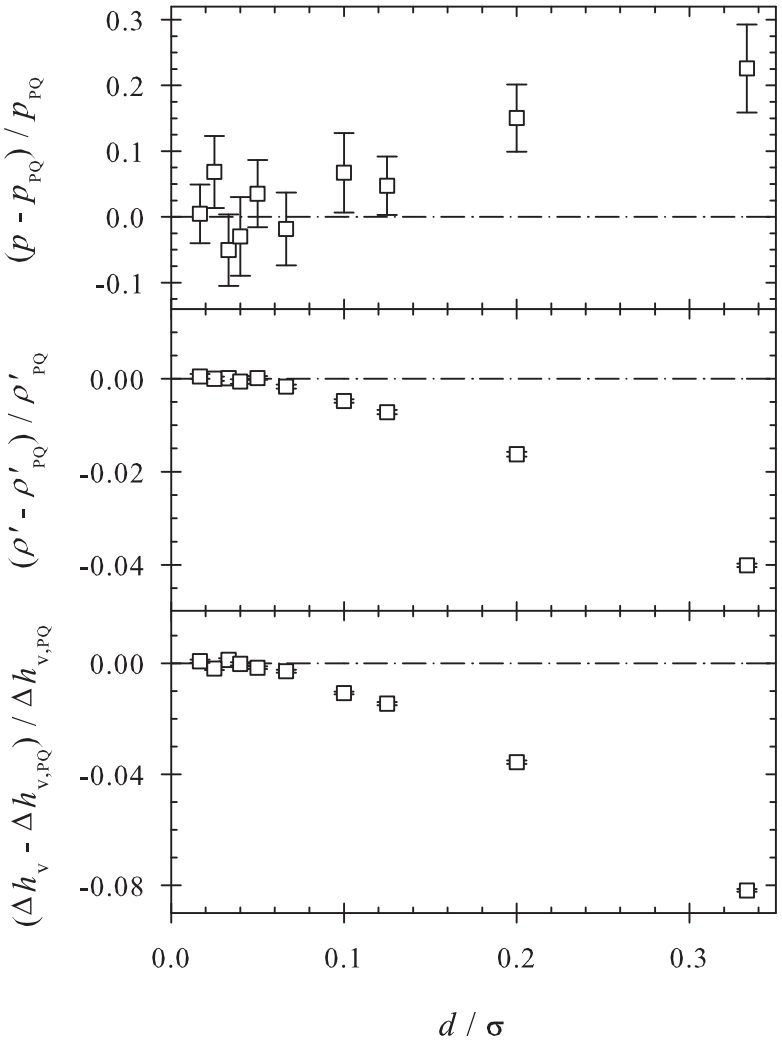

Figure 2. Relative deviations of VLE properties between the point quadrupole (subscript PQ) and the corresponding point charge model for 1,2-Dichloro-1,1,2,2-tetrafluoroethane (CF_2Cl-CF_2Cl) at $T/T_c = 0.7$. The deviations are plotted over the separation d between the point charges. The simulations were carried out with the *ms*2 code [10]. Top: vapour pressure, centre: saturated liquid density, bottom: heat of vaporisation.

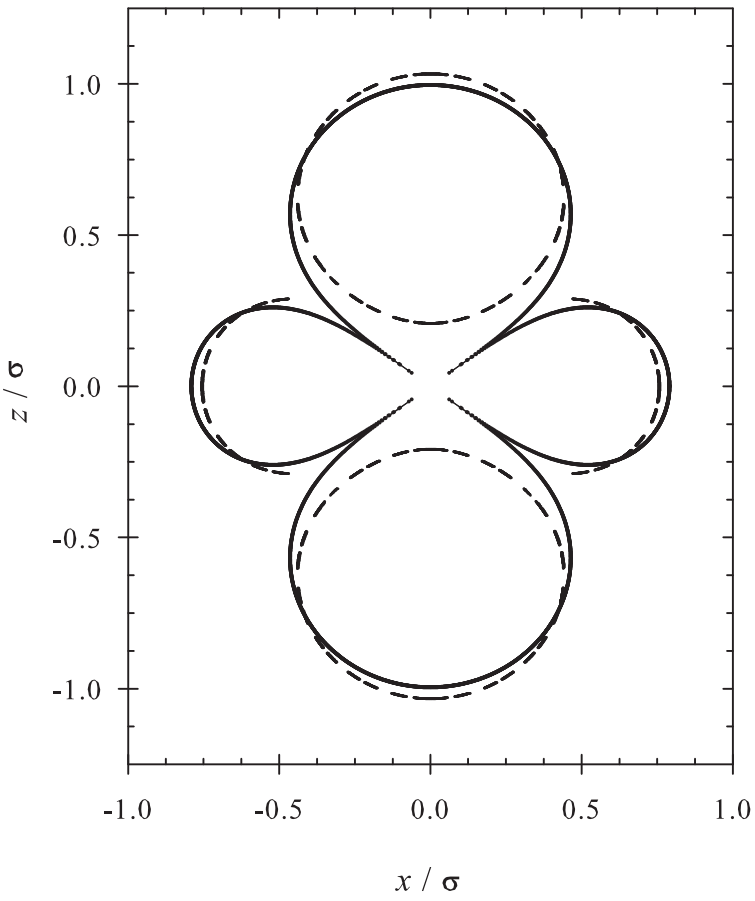

Figure 3. An equipotential line of a point quadrupole and a corresponding linear point charge arrangement with $d/\sigma = 1/3$. Both electrostatic models are oriented along the z-axis, which is the spatial symmetry axis. Solid line: point quadrupole, dashed line: point charge arrangement.

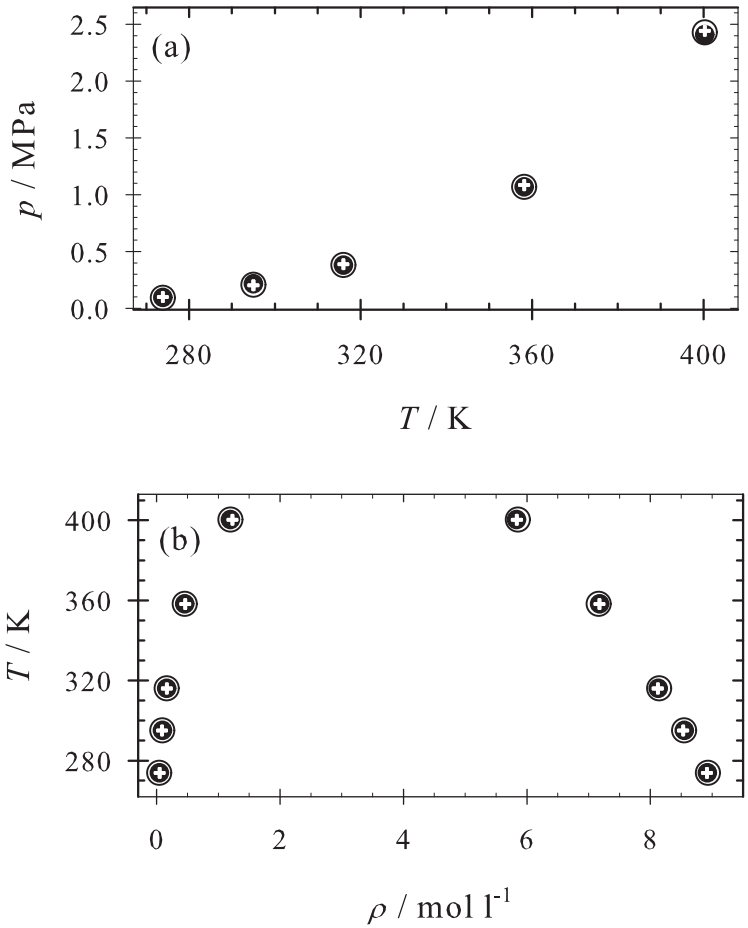

Figure 4. VLE data for 1,2-Dichloro-1,1,2,2-tetrafluoroethane (CF_2Cl-CF_2Cl). The figures show the results of the original model with a point quadrupole (open circle) compared to the results of corresponding models with point charges (full circle: $d/\sigma = 1/20$, empty cross: $d/\sigma = 1/15$): (a) vapour pressure, (b) saturated densities. The simulations were carried out with the *ms*2 code [10].

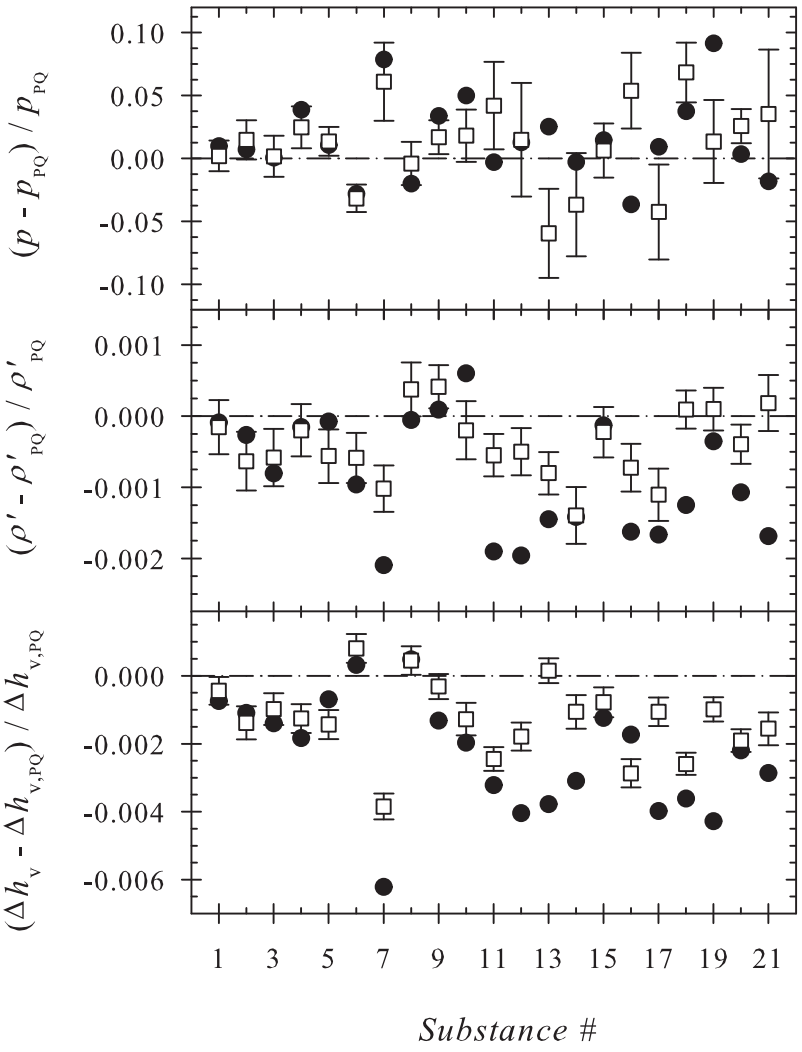

Figure 5. Relative deviations of VLE properties between the point quadrupole model (subscript PQ) and the corresponding point charge model at $T/T_c = 0.7$ for 21 fluids (cf. Table 1) and for two different point charge separations d. The simulations were carried out with the $ms2$ code [10]. Full symbols: $d/\sigma = 1/15$, empty symbols: $d/\sigma = 1/20$. Note that the error bars accompanying the full symbols were omitted for clarity. Top: vapour pressure, centre: saturated liquid density, bottom: heat of vaporisation.

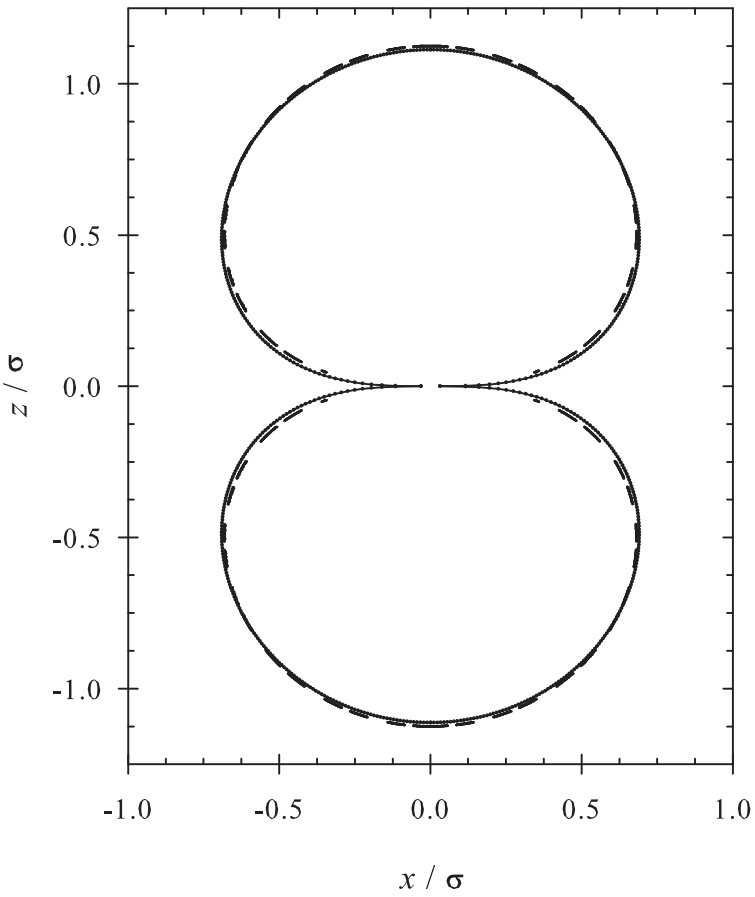

Figure 6. An equipotential line of a point dipole and a corresponding linear point charge arrangement with $d/\sigma = 1/3$. Both electrostatic models are oriented along the z-axis, which is the spatial symmetry axis. Solid line: point dipole, dashed line: point charge arrangement.

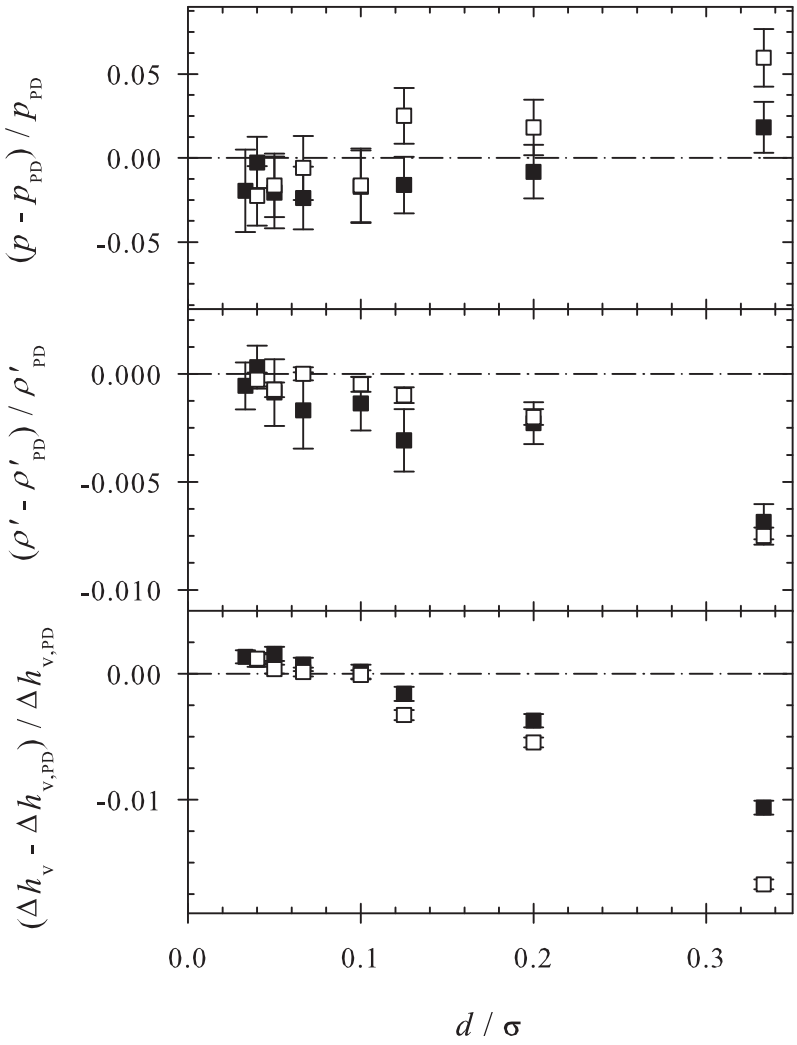

Figure 7. Relative deviations of VLE properties between the point dipole model (subscript PD) and the corresponding point charge model for 1,1-Difluoroethylene (CF_2=CH_2) at $T/T_c = 0.7$. The deviations are plotted over the separation d between the point charges. Full symbols: GEMC code [16], empty symbols: *ms*2 code [10]. Top: vapour pressure, centre: saturated liquid density, bottom: heat of vaporisation.

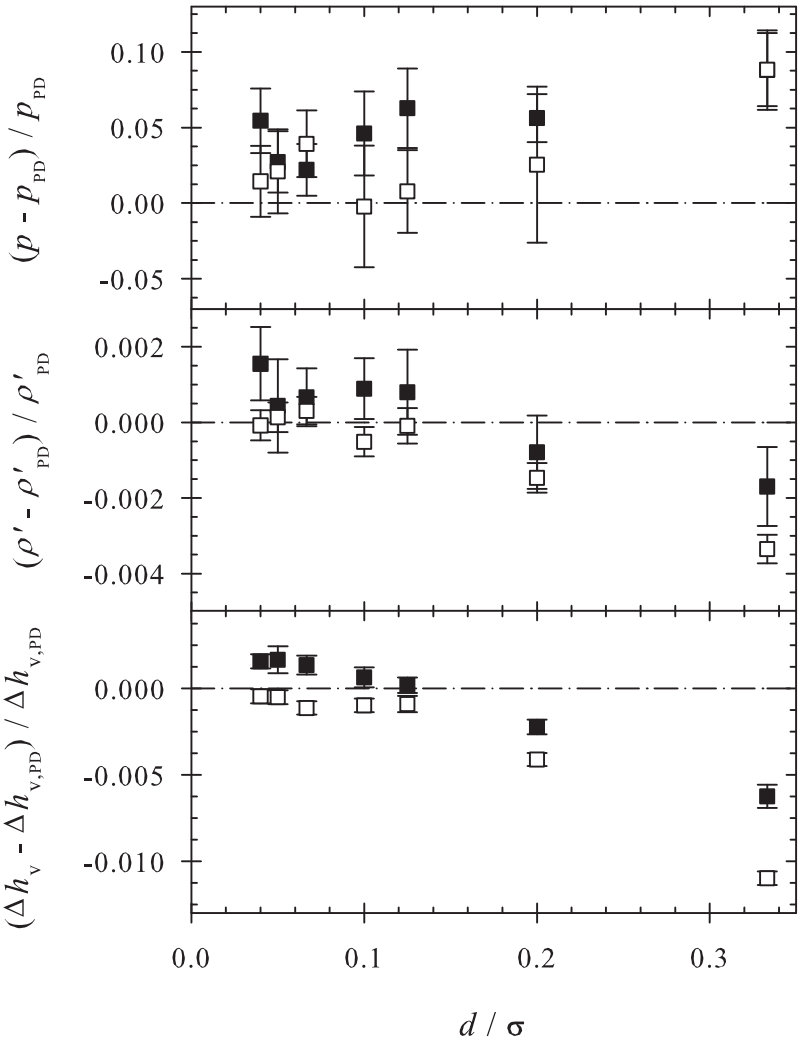

Figure 8. Relative deviations of VLE properties between the point dipole model (subscript PD) and the corresponding point charge model for 1,1,1-Trifluoro-2-bromo-2-chloroethane (CF_3-CHClBr) at $T/T_c = 0.7$. The deviations are plotted over the separation d between the point charges. Full symbols: GEMC code [16], empty symbols: $ms2$ code [10]. Top: vapour pressure, centre: saturated liquid density, bottom: heat of vaporisation.

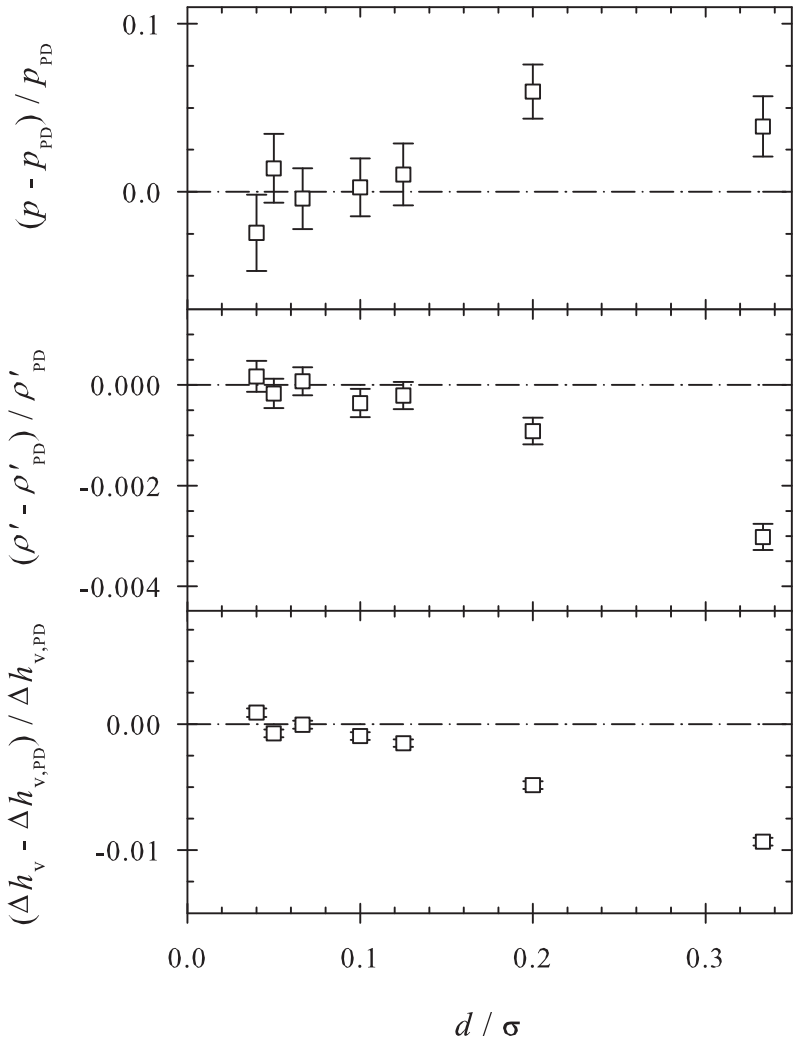

Figure 9. Relative deviations of VLE properties between the point dipole model (subscript PD) and the corresponding point charge model for Methylchloride (CH_3Cl) at $T/T_c = 0.7$. The deviations are plotted over the separation d between the point charges. The simulations were carried out with the *ms*2 code [10]. Top: vapour pressure, centre: saturated liquid density, bottom: heat of vaporisation.

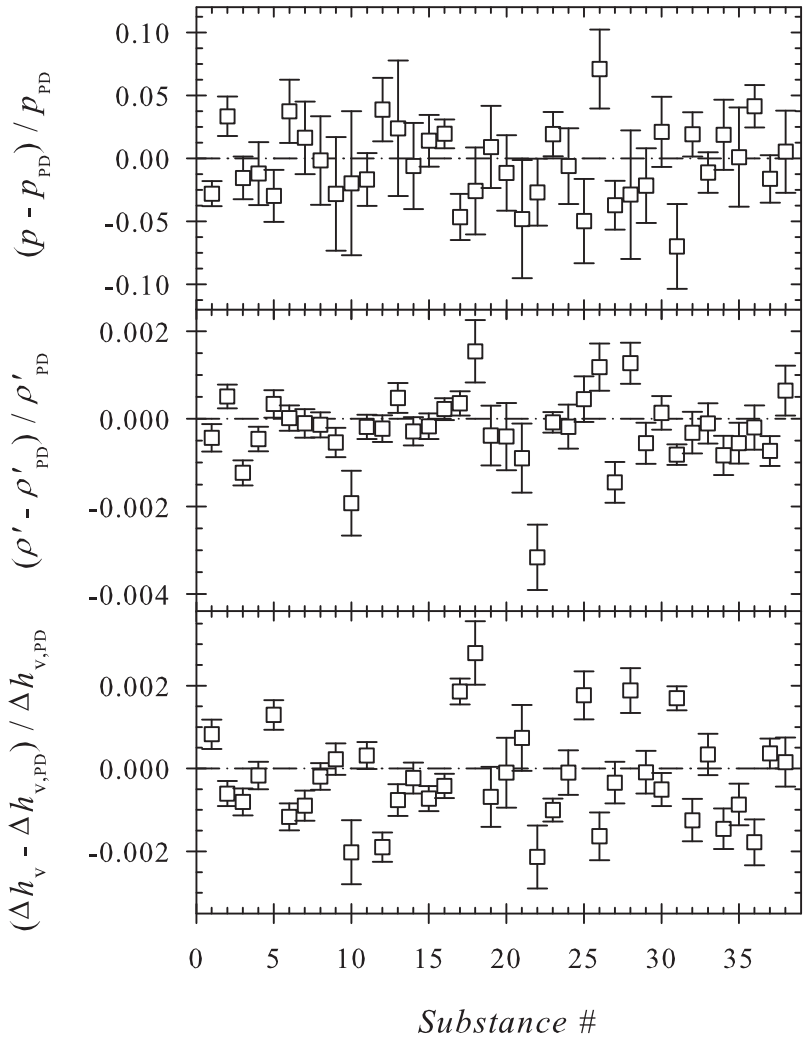

Figure 10. Relative deviations of VLE properties between the point dipole model (subscript PD) and the corresponding point charge model at $T/T_c = 0.7$ for 38 fluids (cf. Table 2) and for a point charge separation of $d/\sigma = 1/20$. The simulations were carried out with the $ms2$ code [10]. Top: vapour pressure, centre: saturated liquid density, bottom: heat of vaporisation.